Hydrophobic Hydration of Amphipathic Peptides

Yuen-Kit Cheng, Wen-Shyan Sheu, and Peter J. Rossky
Department of Chemistry and Biochemistry, University of Texas at Austin, Austin, Texas 78712-1167 USA

ABSTRACT Biomolecular surfaces and interfaces are commonly found with apolar character. The hydrophobic effect thus plays a crucial role in processes involving association with biomolecular surfaces in the cellular environment. By computer simulation, we compared the hydrogen bonding structures and energetics of the proximal hydration shells of the monomer and dimer from a recent study of an extrinsic membrane peptide, melittin. The two peptides were studied in their amphipathic α-helical forms, which possess extended hydrophobic surfaces characterized by different topography. The topography of the peptide-water interface was found to be critical in determining the enthalpic nature of hydrophobic hydration. This topographical dependence has far-reaching implications in the regulation of bioactivities in the presence of amphipathicity. This result also engenders reconsideration of the validity of using free energy parameters that depend solely on the chemical nature of constituent moieties in characterizing hydrophobic hydration of proteins and biomolecules in general.

INTRODUCTION

Membrane proteins, which function as molecule transporters and chemical signal transducers, are necessary in the early stages of the biological activity cascade. Extrinsic (peripheral) membrane proteins, which often remain close to the membrane surface, are thought to be lipid bilayer-perturbing agents when they are present in elevated surface concentrations and are believed responsible for subsequently induced lysis (Matsuzaki et al., 1995; Tytler et al, 1995). In contrast, intrinsic (integral) membrane proteins are relatively large and usually span the width of membranes (von Heijne, 1994; Mouritsen and Bloom, 1993; Stowell and Rees, 1995). Amphipathicity–the segregation of apolar/hydrophobic from polar or charged groups–appears to be a common structural feature of these proteins that is pivotal in understanding the biological mechanism of membrane proteins. At a fundamental level, the hydrophobic interaction of membrane proteins with the hydrocarbon interior of membranes is an important element in the mechanistic interpretation (insertion, translocation, or channel formation) of the biological function of membrane proteins. Therefore, the stability of an amphipathic motif or the propensity for its formation in solution is indispensable in unraveling the mechanistic picture. In the present study, the hydration of amphipathic peptides was investigated. Specifically, the monomeric and dimeric (hypothetical) forms of the extrinsic membrane peptide melittin (Dempsey, 1990) have been chosen to represent amphipathic solutes of contrasting surface topography. The major results for the dimer have been reported recently (Cheng and Rossky, 1998). We focus here on the structural and energetic properties of the proximal solvation shell around hydrophobic groups and specifically on their dependence on surface topography. After describing the peptide models and the methods of study, the results of the two peptide systems are compared and the dependence on surface topography of hydrophobic hydration is discussed. This is followed by discussion of the biological implication of this work.

Model systems

Melittin is a hexacosapeptide found in honey bee venom (Dempsey, 1990). Figure 1 displays surface renderings generated using the program GRASP (Nicholls et al., 1991). Although it is a toxin, when folded it suitably represents one of the most important structural motifs found in membrane proteins, the amphipathic α-helix (Fig. 1 *a*). In an aqueous solution of high peptide concentration, high pH value, or high ionic strength, tetrameric melittin of high symmetry is formed readily (Dempsey, 1990). The tetramer crystal (Terwilliger and Eisenberg, 1982) is a dimer of two almost stereochemically identical dimers related by a twofold symmetry axis (Fig. 1 *b*). The hydrophobic surface of each amphipathic α-helical monomer is essentially completely removed from solvent exposure upon tetramerization (Fig. 1, *a* and *b*). The amino acid sequence of melittin is displayed in Fig. 1 *c*; five of the residues are basic. Distinctively, a nearly flat (slightly concave) surface is located at the center of the dimer that is not found in the monomer (Fig. 1, *a* and *c*). In a recent study, the hydrogen bonding of the hydration shell near that flat surface was shown to be characterized by an enthalpic component that is significantly different from those of water molecules around the convex surface patches of the same molecule (Cheng and Rossky, 1998). In comparison, the hydrophobic surface of the melittin monomer, considered here in addition to the dimer, is a long but narrow strip of contiguous convex patches. This surface topography lies between those of the flat surface and the convex patches of the dimer.

METHODS

We have performed molecular dynamics (MD) simulations for the melittin monomer and the dimer in a solvent box of molecular water at 300 K using

Received for publication October 16, 1998 and in final form January 20, 1999.

Dr. Sheu's current address: Department of Chemistry, Fu-Jen University, Hsin Chuang, Taipei, 242, Taiwan.

Address reprint requests to Yuen-Kit Cheng or Peter J. Rossky, Department of Chemistry and Biochemistry, University of Texas at Austin, Austin, Texas 78712-1167. Tel.: 512-471-3555; Fax: 512-471-1624; e-mail: rossky@mail.utexas.edu.

0006-3495/99/04/1734/10 $2.00

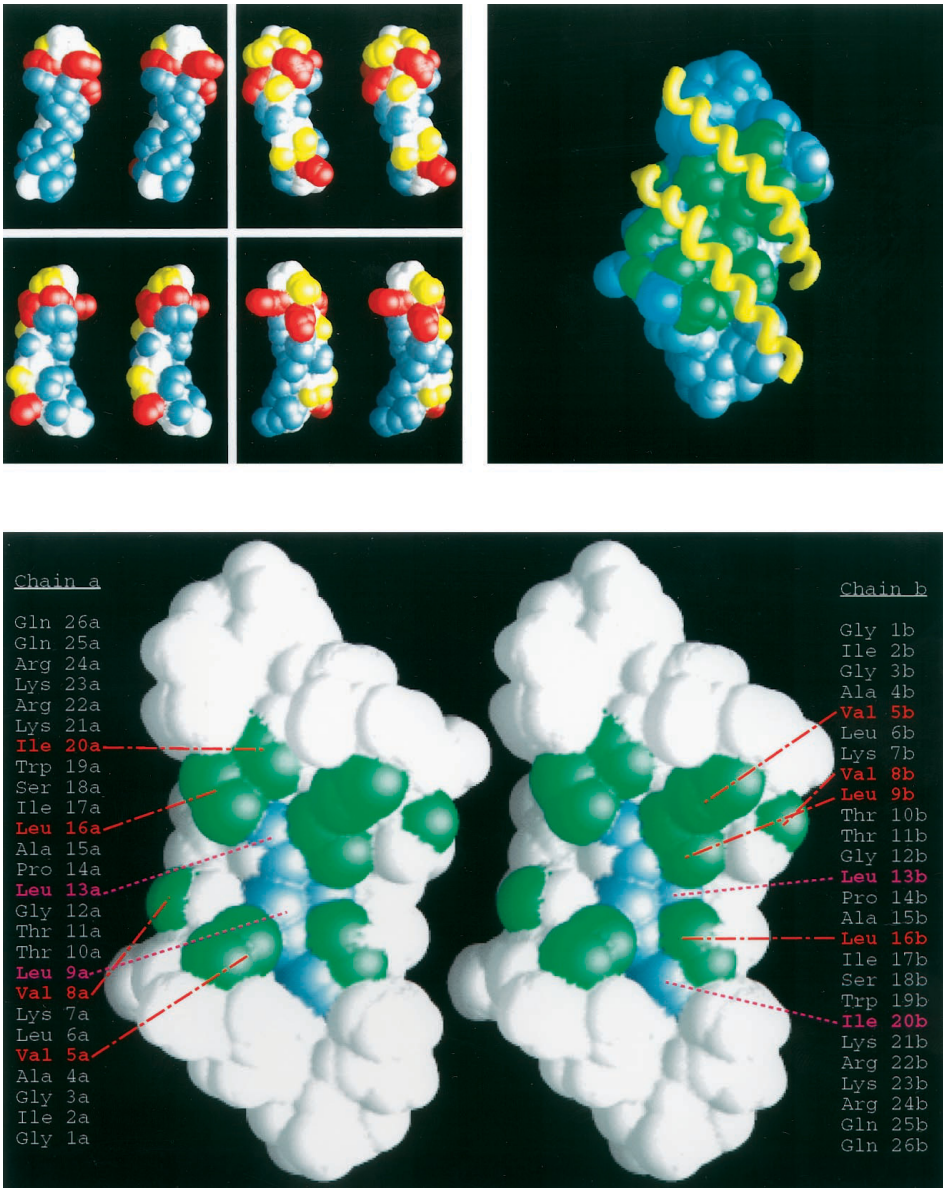

FIGURE 1 Surface topography of melittin monomer, dimer and tetramer in stereoimages. (*a, upper left*) The monomer in amphipathic α-helical form. These four views (generated by successive 90° rotations along the helical axis) of solvent-accessible surface area are displayed with the hydrophobicity of side chains (blue, hydrophobic, including trp; red, charged; yellow, polar; white, gly). The hydrophobic side is a contiguous long strip of convex patches (blue). Each view is oriented so that the N-terminus of melittin helix is at the top. The cluster of the four basic residues (Lys 21a, Arg 22a, Lys 23a, and Arg 24a) is easily seen from the hydrophilic side. (*b, upper right*) Symmetry of the tetramer. Each monomer of the tetramer is amphipathic α-helical. One dimer is rendered as solvent accessible surface (blue) with hydrophobic interface facing out of the page. Hydrophobic side chains are green. For clarity, the other dimer is displayed as helical worms (yellow) along the peptide backbone α-carbon atoms. The hydrophobic interface of this dimer is facing the first one. In each dimer, the two melittin monomers are anti-parallel to each other. (*c*) Hydrophobic surface of the dimer. This solvent-accessible surface is almost completely buried on tetramerization (Terwilliger and Eisenberg, 1982). The peptide sequences are given in standard notations. The central blue contiguous segment is relatively flat and slightly concave (accessible surface area 72.4 $Å^2$) and the convex surface patches are green. Atomic coordinates are adopted from the x-ray crystal structure of the tetramer (Terwilliger and Eisenberg, 1982; Brookhaven Protein Data Bank entry 2MLT). The molecule labeled chain **a** is taken as the monomer. All surface renderings are done by the program GRASP (Nicholls et al., 1991) using a solvent probe radius of 1.4 Å and accessible surface area calculations by GEPOL93 (Pascual-Ahuir et al., 1994).

periodic boundary conditions. Proximal or first solvation shells of the monomer and dimer surfaces were studied in terms of the solvent molecular orientations and binding energetics. For consistent comparison, the atom set selected from the monomer, constituting the relevant surface, is essentially the same set as that of chain **a** in the dimer (Fig. 1 *c*).

Simulations

The method from our previous simulation of hydration of the melittin dimer (Cheng and Rossky, 1998) was adopted here for the melittin monomer, and the results of the former simulation were also used for comparison

and discussion. All of the simulations were performed at a temperature of 300 K in the microcanonical ensemble with cubic periodic boundary conditions, and the spherical cutoff (12Å) minimum image convention for interactions was applied. Trajectories were propagated using the Verlet algorithm (Verlet, 1967) and the simple point charge model (Berendsen et al., 1981); water internal geometry was maintained by employing the SHAKE algorithm (Ryckaert et al., 1977). The x-ray crystal structure of the melittin tetramer (Terwilliger and Eisenberg, 1982) deposited in the Brookhaven Protein Data Bank (Bernstein et al., 1977) was used in our simulations, and the coordinates of one of the two almost identical dimer units were extracted for our study here. Each dimer consists of two chains, **a** and **b**, and chain **a** was selected arbitrarily as the monomer. In terms of current simulation practices, the size, shape, and intermolecular interactions of molecular moieties represented by united or explicit aliphatic carbon and hydrogen atoms are similar. From the point of view of hydrophobic solvation, results deriving from these two representations of a hydrophobic surface are qualitatively equivalent. Therefore, only polar hydrogen atoms were represented and accounted for explicitly. As a result, the monomer and dimer systems consist of 255 and 510 explicit atoms, and contain 3109 and 4420 water molecules enclosed in cubic solvent boxes 46.12 Å and 52.00 Å in length, respectively. The surrounding solvent was set up from equilibrated bulk water so that every solute atom is at least 7 Å from the boundary of the central periodic box. In order to neutralize the peptide charges, the one water molecule closest to the charged center of each charged side chain was replaced with a chloride ion. Equilibrations took approximately 17 ps and 23 ps for the monomer and the dimer systems, respectively. A further 254 ps and 120 ps of the corresponding systems were simulated. The last 135 ps of the monomer trajectory and the full 120 ps dimer trajectory were used for the subsequent analyses. Each time step was 2 fs and the configurations were saved at every 10 steps for both systems. Nonbonded Lennard-Jones (L-J) and coulombic interactions were calculated using atomic pairwise additive potentials with a 12-Å distance cutoff. Those for ions (Smith and Pettitt, 1991; Pettitt and Rossky, 1986) and between ion and water (Chandrasekhar et al., 1984) were adopted from previous works. Water-protein interactions are described via optimized potentials for lipid simulations (OPLS) using simple point charges (Jorgensen and Tirado-Rives, 1988). Standard combining rules were used for L-J parameters between water and protein, and between ion and protein.

Solute atom selection

Solvent accessible surface area (ASA) calculation was used in the selection process. The ASA of solute atoms were computed by using the program GEPOL93 (Pascual-Ahuir et al., 1994), which adheres to the ASA definition of Lee and Richards (1971). A probe radius of 1.4Å, and OPLS parameters of protein-water interactions were adopted (Jorgensen and Tirado-Rives, 1988). Atomic contributions to the ASA were first calculated, then atoms of hydrophobic residues (valine, leucine, and isoleucine in the present case) with ASA $\geq$ 20% relative to corresponding individual, fully exposed atoms were selected. All of the ASA values of backbone atoms of the hydrophobic residues turned out to be negligible. For the dimer, we have further included atoms of hydrophobic residues located in the middle of the surface with non-negligible, but $\leq$ 20%, ASA. The result reveals that essentially all the hydrophobic side chains of the monomer are still solvent-accessible in the dimeric form. Table 1 lists the selected atoms, which were classified into two sets, denoted here as flat and convex. The flat set consists of those atoms on the flat or slightly concave portion of the central surface, and the remaining selected atoms belong to the convex patches (Fig. 1 *c*). Both structural and energetic analyses of proximal hydration were carried out and characterized with respect to these two selected sets.

Solvent hydrogen bonds

The water molecules proximal to each of the selected solute atoms were identified using the proximity analysis introduced by Mehrotra and Beveridge (1980). That is, each solvent molecule is uniquely associated with the hydration shell of the closest solute atom within a distance of 4 Å. For each water molecule, we define the two OH bonds and two lone-pair directions of each water molecule, pointing tetrahedrally outward from the oxygen atom, as four hydrogen-bonding (hb) vectors. The solvent orientation with respect to the surface normal is then measured by the angle (θ) between each of its hb vectors and the outward radial direction pointing from the carbon nucleus associated with the surface toward the water oxygen atom. The measurement of the probabilistic distributions of $\cos\theta$ closely correlates with the structure of the hydration shell (Rossky and Karplus, 1979; Zichi and Rossky, 1985; Kuharski and Rossky, 1984). A hypothetical random distribution of solvent molecules would yield a constant value of 0.5. It is easily seen from Fig. 2 that a water molecule belonging to a clathrate-like hydration shell would give a broad maximum around $\cos\theta_t \approx -0.336$ and a sharp rise close to $\cos(0) = 1$, where θ_t is the tetrahedral angle. These values correspond spatially to three of the four hb vectors of each water molecule oriented nearly tangentially to its proximal surface atom, and one vector pointing away. In contrast, water molecules of an inverted hydration shell, which are characterized by a $\cos\theta$ distribu-

TABLE 1 Selected atom sets of melittin monomer and dimer used in proximal hydration analyses

Chain	Flat set	Convex set
a (monomer)	Leu 9: $C_{\delta1}$, $C_{\delta2}$ Leu 13: $C_{\delta1}$, $C_{\delta2}$	Val 5: $C_{\gamma1}$, $C_{\gamma2}$ Val 8: $C_{\gamma1}$ Leu 16: $C_{\delta1}$, $C_{\delta2}$ Ile 20: $C_{\delta1}$, $C_{\gamma1}$*
b	Leu 13: $C_{\delta1}$ Ile 20: $C_{\delta1}$, $C_{\gamma1}$	Val 5: $C_{\gamma1}$, $C_{\gamma2}$ Val 8: $C_{\gamma2}$ Leu 9: $C_{\delta1}$, $C_{\delta2}$ Leu 16: $C_{\delta1}$, $C_{\delta2}$

All selected atoms of monomer belong to one surface set.
*$C_{\gamma2}$ for monomer.

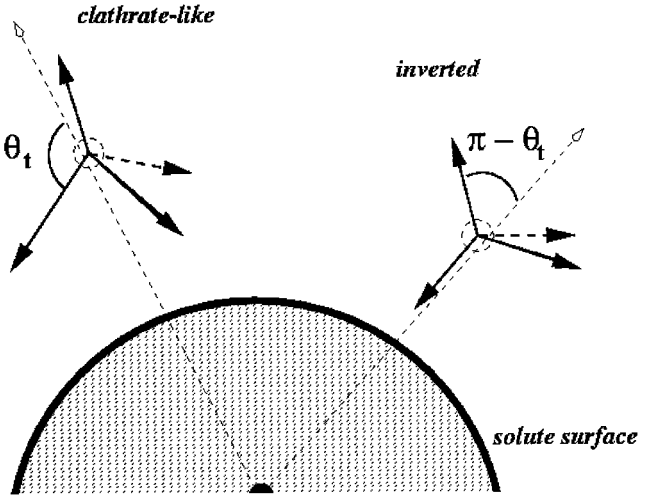

FIGURE 2 Water molecule orientation relative to solute surface normal. Two molecules, each with four equivalent hb vectors, are shown schematically with clathrate-like and inverted orientations, respectively. Of the clathrate-like case, 3 out of 4 of the angles θ (defined in the text) are tetrahedral (θ_t) and the remaining angle is 0°. Such orientation leads to probabilistic distribution of $\cos\theta$ maximizing at -0.336 and 1. In contrast, inverted orientation would lead to a $\cos\theta$ distribution mirroring that of the former and maximizing at -1 and 0.336.

tion maximizing at -1 and at $+0.336$, would have one hb vector pointing directly into the surface, which mirrors that of the clathrate-like one (Fig. 2).

To investigate the degree to which the structural fluctuations are collective contributions from the water molecules, we further consider the quantity f_{in}. This is the ratio of the number of proximal water molecules with any one of its hb vectors pointing radially inward toward the solute atom (defined as $\cos\theta \leq -0.8$) divided by the total number of proximal water molecules of this solute atom found in each configuration. A probability at $f_{in} = 0$ that is higher than that of a hypothetical random orientation would indicate a tendency toward a cage structure formed by a collection of clathrate-like proximal water molecules; collective inversion will render a higher probability at $f_{in} = 1$ than the hypothetical random value. The hypothetical random value is determined analytically by first considering the probability of any given hb vector falling within an appropriate solid angle of 73.7° (corresponding to $\cos\theta \leq -0.8$) with respect to the surface normal, which is 0.1. That is, each proximal water molecule has a random probability value of 0.4 that any one of its four hb vectors points into the surface. Then the quantity f_{in} at each configuration for a hypothetical random orientation can easily be calculated as a binomial probability distribution for the states "in" and "not in," using the known number of proximal water molecules for that configuration. Among the energetic quantities, the average binding energy, E_b (the interaction of a molecule with all other molecules in the system) of proximal water molecules in each surface set is an important one. Except for those proximal water molecules close to the charged peptide termini, the contribution to E_b from water-ion and water-protein interactions are relatively small. Therefore, for further analysis, we first considered only the E_b resulting from the water-water interaction alone, E_{bww}. As another useful quantity for comparison, we also computed the average number of water-water pair interaction energies for a given molecule that are less than or equal to -3.0 kcal mol^{-1}, a number which corresponds to a reasonable definition of the number of hydrogen bonds, $n_{hb(w-w)}$ (Rossky and Karplus, 1979).

RESULTS

For both the melittin monomer and dimer systems, the total intermolecular potential energy of the water-water interaction is -41.1 kJ mol^{-1}, which compares very closely to recent simulations of bulk liquid water using the simple point charge water model (Heyes, 1994; Wallqvist and Teleman, 1991). This indicates that, as expected, any perturbation to water-water interactions caused by the presence of the peptides in the systems (3109 and 4420 water molecules, respectively) is relatively small and most likely local to the solute-water interfaces. It is not surprising that the strong three-dimensional intermolecular network connecting water molecules succeeds in accommodating small hydrocarbon solutes without sacrificing much of its tetrahedral hydrogen bonding (Blokzijl and Engberts, 1993). Other computational studies also show that model solutes of different geometries only perturb the structure and dynamics of water locally (Lee et al., 1984; Wallqvist, 1990; Spohr, 1997). However, as we discuss below, the local perturbation is important and the enthalpic component of water-water interaction of the proximal hydration shell varies significantly with the surface topography of hydrophobic moieties.

Solvent orientation

In Fig. 3, we compared the molecular water orientation relative to the solute surfaces. Proximal water around the monomer clearly resembles the strong clathrate-like hydra-

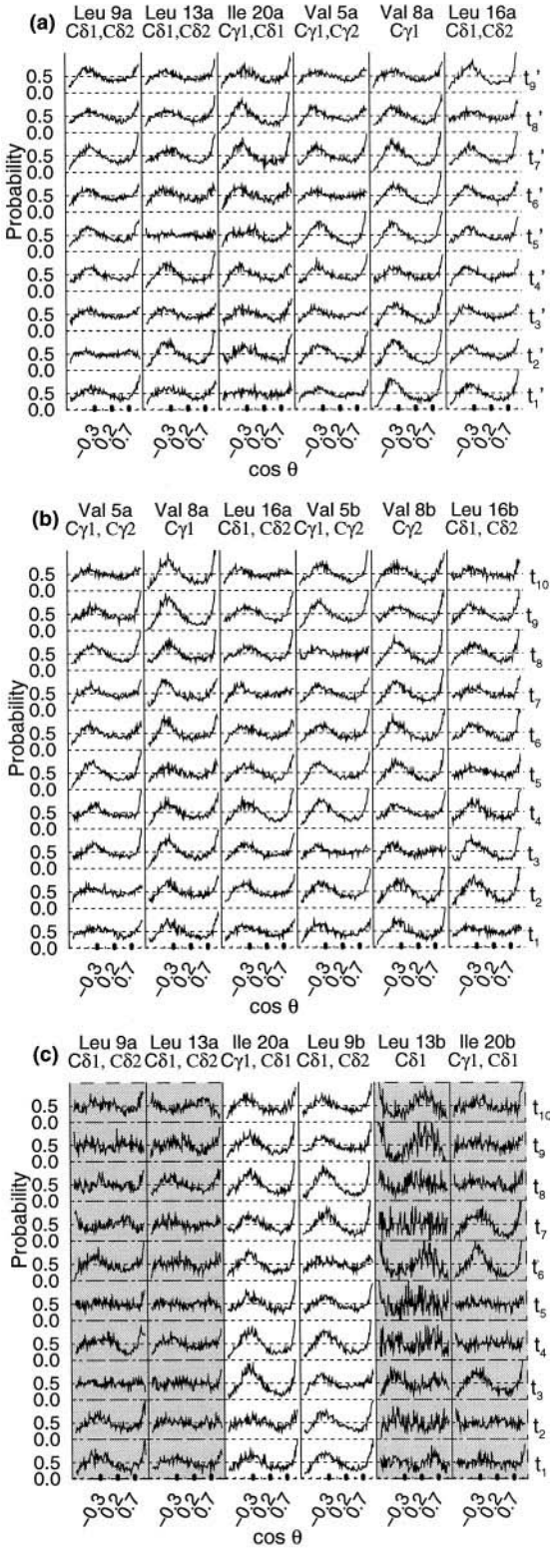

FIGURE 3 Probability distributions of cos θ of proximal water. Each curve is the normalized average of a 15-ps time interval (t_1' to t_9') for the monomer (*a*) or a 12-ps time interval (t_1 to t_{10}) for the dimer (*b* and *c*). Only results of proximal water molecules around selected residues are shown. Results for the flat dimer surface are shaded. Horizontal dotted lines at 0.5 represent the hypothetical result for random solvent orientation. Each cosθ axis is divided into 100 equivalent divisions.

tion shell (Zichi and Rossky, 1985) adopted by the convex surface of the dimer throughout the trajectory (cf. Fig. 3, *a* and *b*). On the other hand, inversion and fluctuation between clathrate and inverted structures are observed in the vicinity of the flat surface of the melittin dimer (Leu 9a, Leu 13a, Leu 13b, and Ile 20b). Because each frame for the dimer represents a 12-ps average, the results for the flat surface of the dimer evidence that any one structural type typically persists for about 10 to 20 ps.

The probabilistic distribution of the quantity f_{in} further illustrates the collective behavior of the water molecules with respect to inversion. Results for a hypothetical random orientation are represented by unfilled bars overlaid adjacent to the corresponding results obtained from simulations. From Fig. 4 *b*, it is obvious that water molecules near the convex surface of the dimer prefer one hydrogen bond pointing away from the surface collectively (high probability at $f_{in} = 0$), corresponding structurally to a hydrogen bond cage (clathrate-like) wrapping around the surface. Notably, solvent around the melittin monomer has the same preferred cage-like hydration shell (Fig. 4 *a*). Water close to the flat surface induced upon dimerization is perhaps not properly discussed in terms of a collective behavior in the current study, because typically only one, or at most two, water molecules are proximal to each individual residue at any time. Nevertheless, the results for f_{in} (Fig. 4 *c*) show that the solvent orientation in this region is best characterized as closer to a random orientation, with that near Leu 13b closer to inverted.

Hydrogen bonding and energetics

There is a prominent difference between the number of water-water hydrogen bonds formed by proximal water of the melittin monomer compared to the dimer. Except for the slight depletion of the probability of forming four hydrogen bonds (Fig. 5 *a*), water molecules proximal to the monomer have similar hydrogen bonding to the bulk, shown as dotted histograms in all graphs in Fig. 5. Water belonging to the proximal hydration shell of the convex surface of the dimer also deviates relatively little from the bulk values. However, as is evident from Fig. 5 *b*, all water molecules proximal to the flat surface of the melittin dimer lose significantly their capability of forming four or even three hydrogen bonds. These patterns of hydrogen bonding capability corroborate the corresponding average binding energies of the proximal water, E_{bww}. The E_{bww} of proximal water belonging to the monomer (-19.60 kcal mol^{-1}) is close to the bulk value except for the residues Val 5a (-17.32 kcal mol^{-1}) and Ile 20a (-17.56 kcal mol^{-1}), which are relatively close to the charged termini with neutralizing chloride ions. Actually, if we also include the water-ion and water-protein interactions, the total binding energies of proximal water for the monomer are $\geq$95% that of the bulk in all cases. The convex hydrophobic surface of the dimer is also characterized by proximal water with a binding energy close to the bulk value. In contrast, for those water molecules of the dimer proximal to the flat surface (Leu 9a, Leu 13a, Leu 13b, and Ile 20b), the average E_{bww} (73–87% of the bulk value) is never close to the bulk value or to the other two surface sets. Notably, in the proximity of Leu 13b, the time-averaged magnitude of E_{bww} decreases by 25% relative to the bulk, a distinctly less favorable result energetically.

From these results we observe that, in general, the breakdown of clathrate-like structure for proximal water correlates with less favorable binding energy and decreasing hydrogen bonding capability.

Can random bulk water describe hydration of a flat hydrophobic surface?

As the results above clearly show, water molecules in the neighborhood of small and convex hydrophobic surface regions prefer clathrate-like orientation. Any other orientation at the surface entails unavoidable loss in the interconnecting tetrahedral hydrogen bonds found in bulk water. Relatively flat surfaces lead to destabilization of clathrate-like structures and to structural fluctuation in the proximal hydration shell. The fluctuating structure on average occasionally resembles hypothetical random fluctuation (flat $\cos\theta$ curves) (see Figs. 3 *c* and 4 *c*). It is relevant to ask whether this random fluctuation is consistent with solvation which is, in fact, uncorrelated with the surface structure in any way other than by that associated simply with the excluded volume of the solute. Equivalently, we can ask if pure bulk water (without the structural readjustment) accommodates a flat hydrophobic surface with a proximal hydration shell having characteristics similar to that observed in the full and complete description. We can address this by inserting solutes into equilibrated pure water, simply removing the now excluded solvent molecules, and then repeating the structural and energetic analyses. Water molecules within 2.950 Å (based on the radial distribution of the water oxygen atom of the actual hydrated systems studied above) of the solute were considered as superimposed on the excluded volume of the solutes and were removed in the calculations. The distance is computed from the center of the water oxygen nucleus to the nucleus of the solute carbon atom.

Selected results for averages taken over relatively short trajectories are shown in Fig. 6. The orientation of the proximal water fluctuates essentially randomly, as expected. Further comparison of these results with the simulated results demonstrates that the hydration structure in the simulation is not simply a random structure. For Leu 13 and Val 8 of the monomer and Val 8a and 8b of the dimer, the result in Fig. 6 fails to show the consistent clathrate structure manifest in Fig. 3. For Leu 13b of the dimer, the regular distributions showing occasional inversion (Fig. 3c) are also not reproduced by the sampled random distribution. The percentages given in each panel correspond to the binding energies (only between water molecules) of the proximal

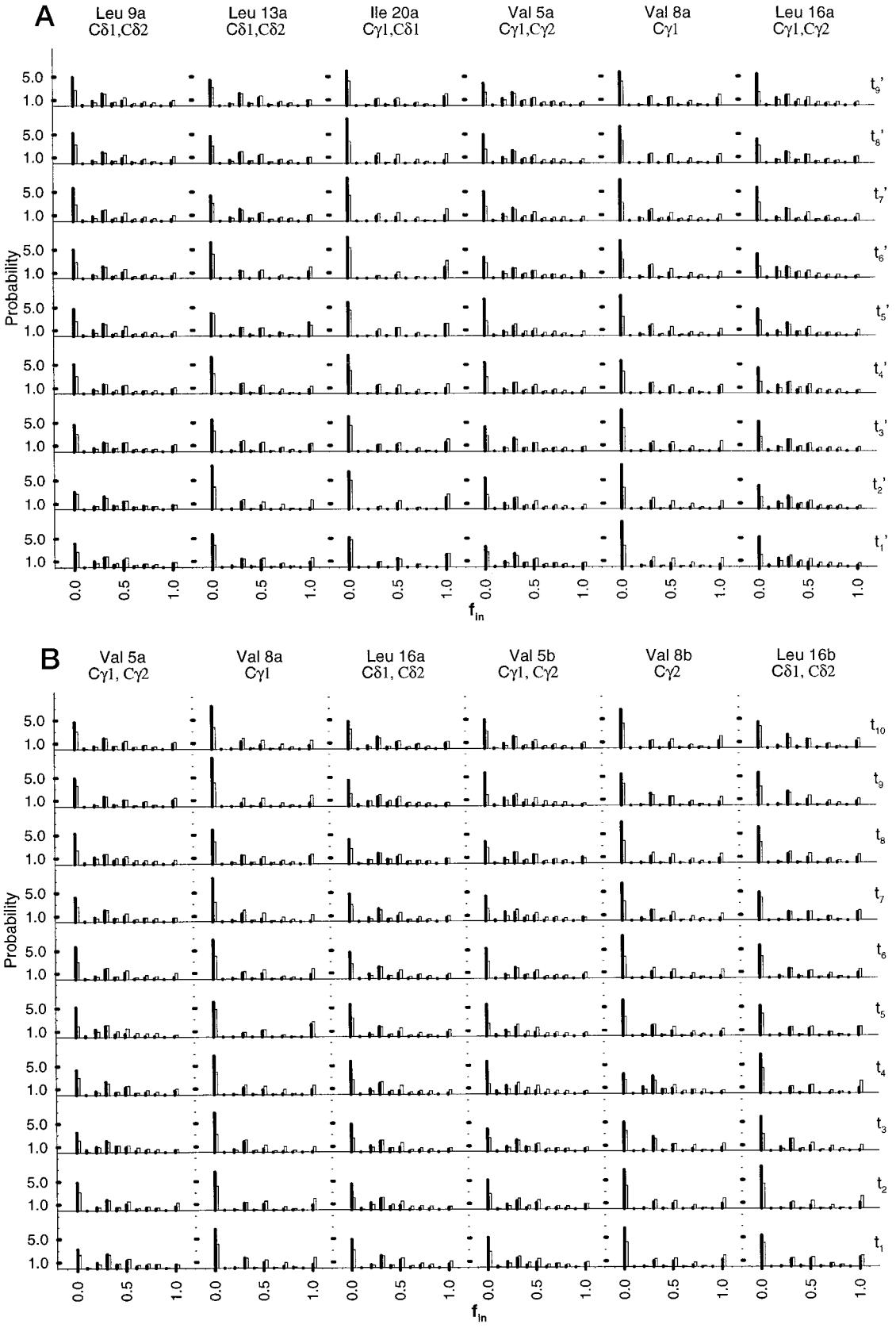

FIGURE 4 Probability distributions of f_{in} of proximal water. All plots are integrally normalized. Unfilled bars represent analytical results for an otherwise random orientation on the same surface and with the same number of proximal water molecules. Results are for monomer (*a*) and dimer (*b* and *c*). Notation is the same as in Fig. 3. Each *x* axis is divided into 10 equivalent divisions.

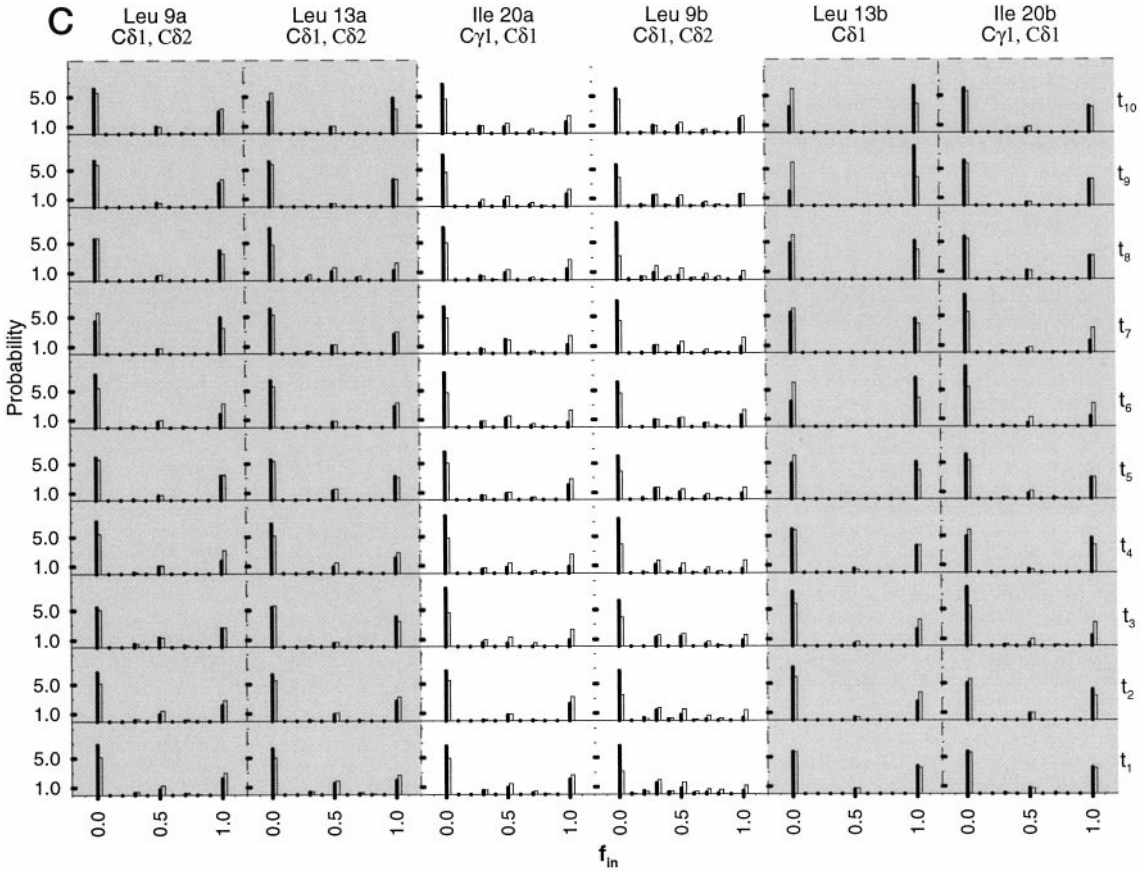

FIGURE 4 Continued

water shell compared with the bulk value, and reflect a loss of roughly 20 to 25% relative to the bulk around convex surfaces (e.g., Leu 13 and Val 8 of the monomer and Val 8a of the dimer). For those near the flat surface of the dimer (e.g., Leu 13b), the corresponding loss is about 50%. The latter is 25% more than that of the actually hydrated system (Cheng and Rossky, 1998). Hence, although the random orientation results correlate with the substantial loss in number of hydrogen bonds (Cheng and Rossky, 1998) and the decrease in the number of proximal water molecules compared with the actual hydrated systems, the observed binding energies here also show that the orientation of the water proximal to either the convex or the flat hydrophobic surface in the actual hydrated systems is not compatible with a random one.

DISCUSSION

The differences in preferred orientations and binding energies of proximal water obtained from the comparison of melittin monomer and dimer systems leave little doubt that the nature of hydrophobic hydration depends significantly on the solute surface topography. We have observed the existence of two distinct modes of hydration shell structure around the peptides. These modes are distinguished from each other by the water orientation relative to the surface normal and the binding energy resulting from water-water interaction. The binding energy was found to correlate reasonably with the number of hydrogen bonds formed between water molecules. The hydrophobic surfaces of the melittin systems studied here can be broadly classified into three topographical cases: the central, essentially flat, region of the dimer; the isolated and small convex patches of the dimer flanking the flat surface; and the contiguous and long strip of convex patches of the monomer. Our results show that the surfaces for the latter two cases rendered very similar clathrate-like interfacial structure, whereas the flat region shows disruption and inversion. Biomolecules possessing flat hydrophobic surfaces of larger sizes, e.g., the hydrophobic surfaces of chaperones (Braig et al., 1994), are thus of considerable interest in order to probe this aspect more thoroughly.

Throughout the simulations, we intentionally kept the peptide structures rigid and fixed in position in order to investigate cleanly and directly the solute surface topography-dependence of hydration. One can then ask if the observed hydration will provide a force for solute distortion, based on the gradient of the full energy. The melittin molecule in aqueous solution has previously been studied computationally with an emphasis on its dynamics (Kitao et al., 1991). At least superficially, the peptide structure in that report corresponds to the one studied here.

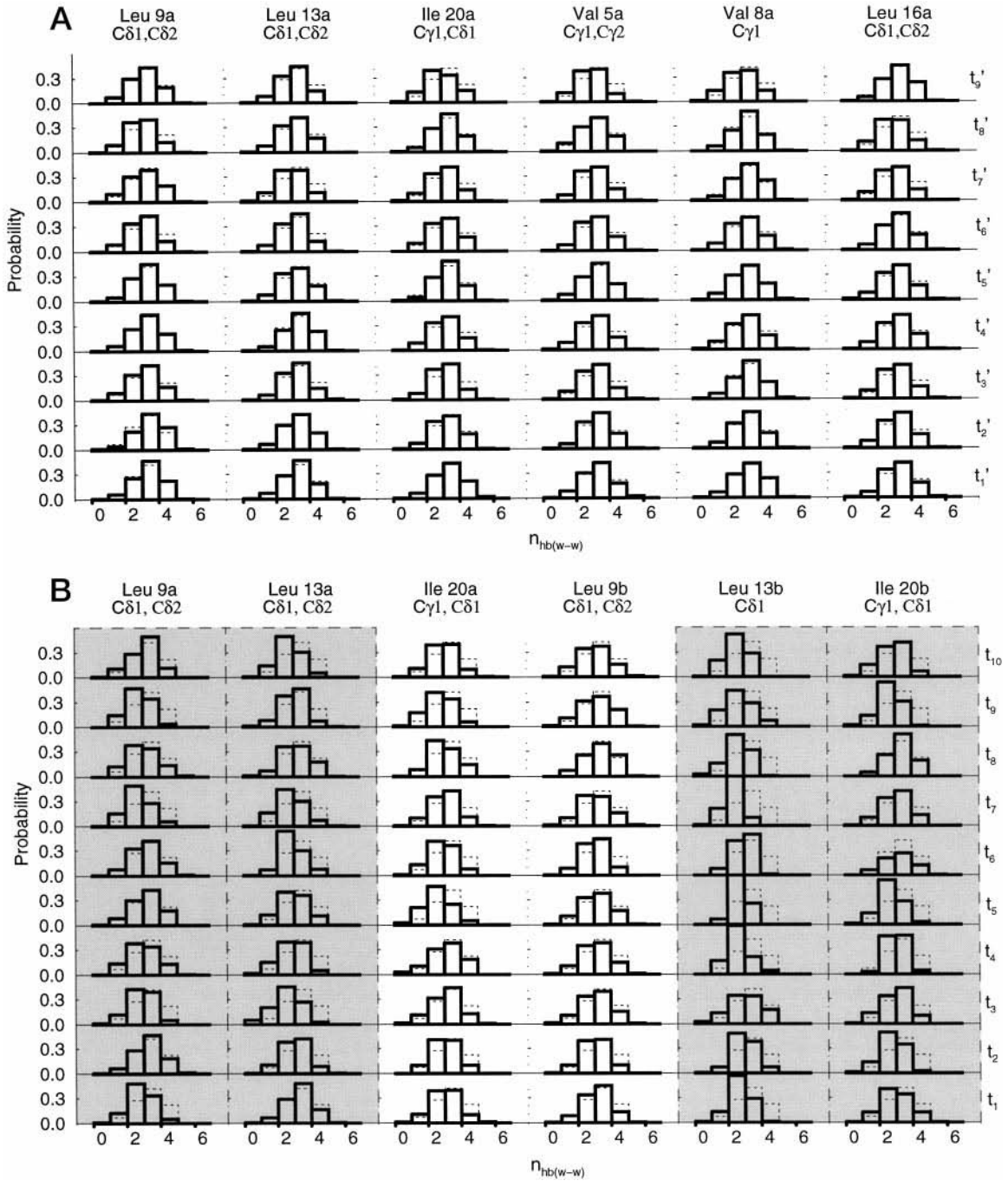

FIGURE 5 Probability distributions of $n_{hb(w-w)}$ of proximal water. Only results for the monomer (*a*) and the dimer flat surface (*b*) are shown. Notation is the same as in Fig. 3.

The ability of melittin to form an amphipathic α-helix in specific solution conditions has been shown experimentally to be critical to its membrane lytic activity, and the disruption of its helix formation results in reducing or voiding activity (Pérez-Payá et al., 1995). Recent studies indicated that at equilibrium in fully solvated membranes, melittin is helical and lies parallel to the surface (Frey and Tamm, 1991; Dempsey and Butler, 1992; Okada et al., 1994). Early nuclear magnetic resonance studies also suggested that its helical axis is parallel to the bilayer surface with the hydrophilic side pointing into the surface (Altenbach et al., 1989). However, it appears that, in general, the orientation and membrane activities of an extrinsic membrane protein depend on its surface concentration, the composition of lipid bilayer, and solution conditions such as pH values (Yuan et al., 1996; Ishiguro et al., 1996; Ohki et al., 1994). Independent of the exact biological mechanism(s) of membrane proteins, hydrophobic hydration must play a crucial role. This view is the consequence of the ubiquitous element–amphipathicity–found in the active process of numerous

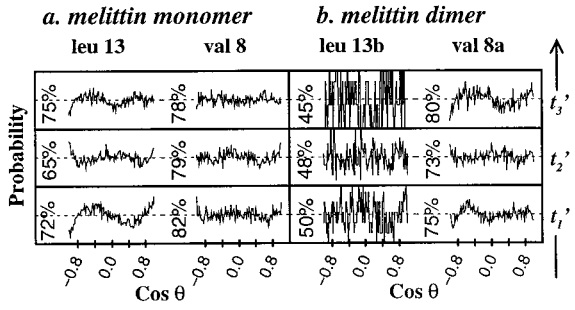

FIGURE 6 Proximal water orientation for solutes in bulk water without structural relaxation for melittin monomer (*a*) and dimer (*b*). Each curve is the normalized average of a 15-ps time interval for the monomer (*a*) or a 12-ps time interval for the dimer (*b*). Each *x* axis is divided into 100 equivalent divisions. The percentage of the corresponding bulk water-water binding energy for proximal water is given next to each curve (*left*).

membrane proteins. A monomeric melittin molecule is only soluble in solution as a random coil (Dempsey 1990), but the amphipathic form appears to be important for its bioactivity. It is reasonable to hypothesize that the concurrent amphipathic helix formation and tetramerization of melittin at physiological conditions acts as a cellular regulating process to deliver the functional form of melittin to the membrane surface. We note that amphipathicity also finds importance in biological systems other than membrane proteins, such as hormones and cofactors (Kaiser and Kezdy, 1984), and it is also considered an important element in the protein folding problem; melittin itself has been studied in this regard (Wilcox and Eisenberg, 1992).

In the context of the current study, the enthalpic dependence of solvent water-binding energy on solute surface topography should be reflected in the heat capacity change upon solute hydration (Madan and Sharp, 1996). This heat capacity change, which is experimentally accessible, is widely accepted as an indicator of hydrophobicity (Madan and Sharp, 1996). Therefore, it would be very valuable if the hydrophobicities of biomolecules with hydrophobic surfaces of comparable solvent accessible surface areas, but possessing convex and flat concave topography, could be measured and compared.

Finally, and perhaps of most importance, hydration free energy calculations based on solvent ASA of biomolecules empirically parameterized with respect to various chemical constituents has become the practice and has led to useful predictions (Eisenberg and McLachlan, 1986; Spolar and Record, Jr., 1994). However, there is no a priori basis for broadly applying this sole dependence on solvent ASA and ignoring other factors. For instance, enzymatic processes occur primarily in localized regions, and differences in the hydrophobic hydration resulting from the dependence on the local surface topography should lead to significant differences in the hydration structure and free energetics. The present study clearly elucidates the likely existence of this dependence and should be considered in studies of processes with confined geometry. The extension of this work to hydrophobic surfaces and interfaces which include polar or charged insertions, which is a more general case for biological events, is desirable and will be considered elsewhere.

CONCLUSION

By studying the hydration properties of the interfaces between water and the hydrophobic surfaces of the membrane active peptide melittin in its monomeric and dimeric forms, we have shown that the hydrophobic hydration of biomolecules is substantially dependent on the surface topography. Two distinct modes of proximal hydration structure, clathrate-like and inverted, are observed. These are characterized by a significant difference in the enthalpies of water-water interactions. Further studies, currently underway, on highly concave, hydrophobic surfaces will provide additional generalization of how water responds to nonconvex hydrophobic biomolecular surfaces. Further studies focusing on free energy for the melittin system may elucidate the role of both hydrophobic surfaces and amphipathic motifs in physiological association.

Support of this work by a grant from the National Institutes of Health is gratefully acknowledged. Additional support has been provided by the R. A. Welch Foundation. We also acknowledge T. S. Cohen for contributions in the early stages of this work. Y.-K.C. also cordially thanks K. F. Wong for helpful discussions.

REFERENCES

Altenbach, C., W. Froncisz, J. S. Hyde, and W. L. Hubbell. 1989. Conformation of spin-labeled melittin at membrane surfaces investigated by pulse saturation recovery and continuous wave power saturation electron paramagnetic resonance. *Biophys. J.* 56:1183–1191.

Berendsen, H. J. C., J. P. M. Postma, W. F. van Gunsteren, and J. Hermans. 1981. Interaction models for water in relation to protein hydration. In Intermolecular Forces, (Pullman, B., ed.), Reidel Dordrecht. 331–342.

Bernstein, F. C., T. F. Koetzle, G. J. B. Williams, E. F. Meyer, Jr., M. D. Brice, J. R. Rodgers, O. Kennard, T. Shimanouchi, and M. Tasumi. 1977. The protein data bank: a computer-based archival file for macromolecular structures. *J. Biol. Chem.* 112:535–542.

Blokzijl, W., and J. B. F. N. Engberts. 1993. Hydrophobic effects: opinions and facts. *Angew. Chem. Int. Ed. Engl.* 32:1545–1579.

Braig, K., Z. Otwinowski, R. Hegde, D. C. Boisvert, A. Joachimiak, A. L. Horwich, and P. B. Sigler. 1994. The crystal structure of the bacterial chaperonin GroEL at 2.8Å. *Nature (London).* 371:578–586.

Chandrasekhar, J., D. C. Spellmeyer, and W. L. Jorgensen. 1984. Energy component analysis for dilute aqueous solutions of Li^+, Na^+, F^-, and Cl^- ions. *J. Am. Chem. Soc.* 106:903–910.

Cheng, Y.-K., and P. J. Rossky. 1998. Surface topography dependence of biomolecular hydrophobic hydration. *Nature (London).* 392:696–699.

Dempsey, C. E. 1990. The actions of melittin on membranes. *Biochim. Biophys. Acta.* 1031:143–161.

Dempsey, C. E., and G. S. Butler. 1992. Helical structure and orientation of melittin in dispersed phospholipid membranes from amide exchange analysis in situ. *Biochemistry.* 31:11973–11977.

Eisenberg, D., and A. D. McLachlan. 1986. Solvation energy in protein folding and binding. *Nature (London).* 319:199–203.

Frey, S., and L. K. Tamm. 1991. Orientation of melittin in phospholipid bilayers: a polarized attenuated total reflection infrared study. *Biophys. J.* 60:922–930.

Heyes, D. M. 1994. Physical properties of liquid water by molecular dynamics simulations. *J. Chem. Soc. Faraday Trans.* 90:3039–3049.

Ishiguro, R., M. Matsumoto, and S. Takahashi. 1996. Interaction of fusogenic synthetic peptide with phospholipid bilayers: orientation of the peptide α-helix an binding isotherm. *Biochemistry.* 35:4976–4983.

Jorgensen, W. L., and J. Tirado-Rives. 1988. The OPLS potential functions for proteins: energy minimizations for crystals of cyclic peptides and crambin. *J. Am. Chem. Soc.* 110:1657–1671.

Kaiser, E. T., and F. J. Kezdy. 1984. Amphiphilic secondary structure: design of peptide hormones. *Science.* 223:249–255.

Kitao, A., F. Hirata, and N. Go. 1991. The effects of solvent on the conformation and collective motions of protein: normal mode analysis and molecular dynamics simulations of melittin in water and in vacuum. *Chem. Phys.* 158:447–472.

Kuharski, R. A., and P. J. Rossky. 1984. Solvation of hydrophobic species in aqueous urea solution: A molecular dynamics study. *J. Am. Chem. Soc.* 106:5794.

Lee, B., and F. M. Richards. 1971. The interpretation of protein structures: estimation of static accessibility. *J. Mol. Biol.* 55:379–400.

Lee, C. Y., J. A. McCammon, and P. J. Rossky. 1984. The structure of liquid water at an extended hydrophobic surface. *J. Chem. Phys.* 80: 4448–4455.

Lijnzaad, P., and P. Argos. 1997. Hydrophobic patches on protein subunit interfaces: Characteristics and prediction. *Proteins.* 28:333–343.

Lijnzaad, P., J. C. Berendsen, and P. Argos. 1996. Hydrophobic patches on the surfaces of protein structures. *Proteins.* 25:389–397.

Madan, B., and K. Sharp. 1996. Heat capacity changes accompanying hydrophobic and ionic solvation: a Monte Carlo and random network model study. *J. Phys. Chem.* 100:7713–7721.

Matsuzaki, K., O. Murase, N. Fujii, and K. Miyajima. 1995. Translocation of a channel-forming antimicrobial peptide, magainin 2, across lipid bilayers by forming a pore. *Biochemistry.* 34:6521–6526.

Mehrotra, P. K., and D. L. Beveridge. 1980. Structural analysis of molecular solutions based on quasi-component distribution functions. Application to $[H_2CO]_{aq}$ at 25°C. *J. Am. Chem. Soc.* 102:4287–4294.

Mouritsen, O. G., and M. Bloom. 1993. Models of lipid-protein interactions in membranes. *Annu. Rev. Biophys. Biomol. Struct.* 22:145–171.

Nicholls, A., K. A. Sharp, and B. Honig. 1991. Protein folding and association: insights from the interfacial and thermodynamic properties of hydrocarbons. *Proteins.* 11:281–296.

Ohki, S., E. Marcus, D. K. Sukumaran, and K. Arnold. 1994. Interaction of melittin with lipid membranes. *Biochim. Biophys. Acta.* 1194:223–232.

Okada, A., K. Wakamatsu, T. Miyazawa, and T. Higashijima. 1994. Vesicle-bound conformation of melittin: transferred Nuclear Overhauser Enhancement analysis in the presence of perdeuterated phosphatidylcholine vesicles. *Biochemistry.* 33:9438–9446.

Pascual-Ahuir, J. L., Silla, E. and Tunon, I. 1994. GEPOL: An improved description of molecular surfaces. III. A new algorithm for the computation of the solvent-excluding surface. *J. Comput. Chem.* 15: 1127–1138.

Pérez-Payá, E., R. A. Houghten, and S. E. Blondelle. 1995. The role of amphipathicity in the folding, self-association and biological activity of multiple subunit small proteins. *J. Biol. Chem.* 270:1048–1056.

Pettitt, B. M., and P. J. Rossky. 1986. Alkali halides in water: ion-solvent correlations and ion-ion potentials of mean force at infinite dilution. *J. Chem. Phys.* 84:5836–5844.

Rossky, P. J., and M. Karplus. 1979. Solvation: a molecular dynamics study of a dipeptide in water. *J. Am. Chem. Soc.* 101:1913–1937.

Ryckaert, J.-P., G. Ciccotti, and H. J. C. Berendsen, 1977. Numerical integration of the Cartesian equations of motion of a system with constraints: molecular dynamics of *n*-alkanes. *J. Comput. Phys.* 23: 327–341.

Smith, P. E., and B. M. Pettitt. 1991. Effects of salt on the structure and dynamics of the bis(penicillamine) enkephalin zwitterion: A simulation study. *J. Am. Chem. Soc.* 113:6029–6037.

Spohr, E. 1997. Molecular dynamics simulation studies of the density profiles of water between (9–3) Lennard-Jones walls. *J. Chem. Phys.* 106:388–391.

Spolar, R. S., and M. T. Record, Jr. 1994. Coupling of local folding to site-specific binding of proteins to DNA. *Science.* 263:777–784.

Stowell, M. H. B., and D. C. Rees. 1995. Structure and stability of membrane proteins. *Adv. Protein Chem.* 46:279–311.

Terwilliger, T. C., and D. Eisenberg. 1982. The structure of melittin. I. Structure determination and partial refinement. *J. Biol. Chem.* 257: 6010–6015.

Tsai, C.-J., S. L. Lin, H. J. Wolfson, and R. Nussinov. 1997. Studies of protein-protein interfaces: a statistical analysis of the hydrophobic effect. *Protein Sci.* 6:53–64.

Tytler, E. M., G. M. Anantharamaiah, D. E. Walker, V. K. Mishra, M. N. Palgunachari, and J. P. Segrest. 1995. Molecular basis for prokaryotic specificity of magainin-induced lysis. *Biochemistry.* 34:4393–4401.

Verlet, L. 1967. Computer "experiments" on classical fluids. I. Thermodynamical properties of Lennard-Jones molecules. *Phys. Rev.* 159: 98–103.

von Heijne, G. 1994. Membrane proteins: from sequence to structure. *Annu. Rev. Biophys. Biomol. Struct.* 23:167–192.

Wallqvist, A. 1990. Polarizable water at hydrophobic wall. *Chem. Phys. Lett.* 165:437–442.

Wallqvist, A., and O. Teleman. 1991. Properties of flexible water models. *Mol. Phys.* 74:515–533.

Wilcox, W., and D. Eisenberg. 1992. Thermodynamics of melittin tetramerization determined by circular dichroism and implications for protein folding. *Protein Sci.* 1:641–653.

Yuan, P., P. J. Fisher, F. G. Prendergast, and M. D. Kemple. 1996. Structure and dynamics of melittin in lysomyristoyl phosphatidylcholine micelles determined by nuclear magnetic resonance. *Biophys. J.* 70: 2223–2238.

Zichi, D. A., and P. J. Rossky. 1985. The equilibrium solvation structure for the solvent-separated hydrophobic bond. *J. Chem. Phys.* 83: 797–808.